FRACTURE BEHAVIOUR OF A NEW SUBMICRON GRAINED CEMENTED CARBIDE

F.A. COSTA OLIVEIRA[1,2]*, A.C. LOPES[2], J. CRUZ FERNANDES[2], J. SACRAMENTO[3], M.A. VALENTE[3]

[1] Departamento de Materiais e Tecnologias de Produção, INETI, I.P., Estrada do Paço do Lumiar, 1649-038 Lisboa, Portugal.
[2] Departamento de Engenharia de Materiais, Instituto Superior Técnico, Av. Rovisco Pais, 1049-001 Lisboa, Portugal.
[3] DURIT Metalurgia Portuguesa do Tungsténio Lda., Apartado 24P, 3850 Albergaria-A-Velha, Portugal.
fernando.oliveira@ineti.pt

ABSTRACT: In this work, the effect of increasing argon pressure applied on a post-sintering treatment from 3 MPa to 100 MPa on the mechanical properties of a newly developed hardmetal grade, namely, hardness, flexural strength and fracture toughness, is reported. The as-received material has been previously sintered at 1460ºC under 2 MPa argon pressure from powder mixtures of WC and 3.5 wt% Co together with minor additions of VC, graphite and a pressing lubricant.

By increasing the argon pressure, a significant increase in flexural strength from ≈ 1500 MPa to ≈ 3000 MPa was observed, whilst hardness (HV30≈2000) and fracture toughness (≈8 $MN.m^{-3/2}$) remained practically unchanged. Both microstructural and fractographic studies revealed that this is mainly attributed to a decrease in the amount and size of microstructural defects (namely, pores and metallic inclusions). Furthermore, fracture has been found to occur mainly by intrinsic (bulk) defects rather than surface-related ones, suggesting that surface finishing did not affect flexural strength measurements.

Hot isostatic pressing has been successfully used to consolidate WC-3.5wt% Co composites with submicron WC grains size confirming that porosity reduction results in flexural strength improvement.

Keywords: Hardmetal; Flexural strength; Fractography; Fracture toughness; Microstructure.

RESUMO: Apresenta-se o estudo do efeito nas propriedades mecânicas de um novo grau de metal duro, em resultado do aumento da pressão de árgon aplicada num tratamento de pós-sinterização. O material foi previamente sinterizado a 1460ºC, à pressão de árgon de 2 MPa, a partir de misturas de pós de WC conjuntamente com 3,5 %p de Co e pequenas adições de VC, grafite e um lubrificante adequado à prensagem.

Registou-se um aumento significativo da resistência à flexão de ≈ 1500 MPa para ≈ 3000 MPa quando se aumentou a pressão de árgon de 3 para 100 MPa, ao mesmo tempo que a dureza (HV30≈2000) e a tenacidade à fractura (≈8 $MN.m^{-3/2}$) permaneceram praticamente inalteradas. Estudos microestruturais e de análise de fractura revelaram que este comportamento se deve fundamentalmente à diminuição da quantidade e do tamanho dos defeitos críticos (nomeadamente, poros e inclusões metálicas). Além disso, observou-se que a fractura ocorre devido a defeitos intrínsecos e não a defeitos de superfície, o que sugere que o acabamento de superfície aplicado não afecta a medida da resistência à flexão.

Constata-se que a prensagem isostática a quente é uma técnica adequada para a obtenção de compósitos de WC-3,5%p Co com tamanho de grão submicrométrico, verificando-se que a diminuição do teor da porosidade residual provoca um notável aumento da resistência à flexão.

Palavras chave: Metal duro; Resistência à flexão; Análise de fractura; Tenacidade à fractura; Microestrutura.

1. INTRODUCTION

Presently, the hardmetal industry is mainly concerned with improving the manufacturing process of finer grained WC-Co hardmetals in order to maximize hardness while keeping a reasonable toughness [1-3]. Submicron cemented carbides are characterised by levels of strength, hardness and wear resistance that lead to long tool life [4,5]. Such very hard materials are required for miniature drills for highly integrated printed circuit boards (PCB), pins for dot-printers, wood machining, dental drills, rock drill buttons as well as other wear resistant parts.

Since hardness and wear increase with decreasing WC grain size, the current trend towards the development of finer and finer-graded cemented carbides requires new manufacturing processes for both powders and grades. Indeed, several authors have shown that an increase in hardness and flexural strength of hardmetals is obtained by reducing WC grain

size below 1 μm. Typically, materials having a grain size in the range 0.5-0.8 μm are referred to as sub-micron grades, whereas hardmetals with a grain size in the 0.2-0.5 μm range are known as ultra-fine [6]. The latest reduction in grain size into <0.2 μm has resulted in the so-called "nano-crystalline" hardmetals [7].
The manufacturing of such finer-grades presents a number of challenges related to the manipulation and pressing of the finer powder mixtures as well as the need of an effective WC grain growth control upon sintering. The latter can be achieved through addition of small amounts of grain growth inhibitors (typically VC and Cr_3C_2) homogeneously distributed in the powder mixtures. However, as the WC grain size decreases the optimum amount of inhibitor increases which is detrimental to fracture toughness [8].
By applying HIP after sintering treatments, several researchers [9, 10] proved that it is possible to eliminate residual porosity of ultrafine grades with an outstanding improvement on the fracture strength and hardness.

The aim of this work was to evaluate the influence of increasing post-sintering argon pressure from 3 to 100 MPa on the mechanical properties, namely hardness, flexural strength and fracture toughness, observed in a newly developed sub-micrometer WC-Co grade with low binder content (3.5 wt% Co) and to provide some light into the fracture mechanisms involved. Despite experimental data already available, several aspects of the mechanical behaviour of WC-Co hardmetals are still not fully understood. In particular, resistance against brittle fracture, so-called "toughness", remains an intriguing issue to be solved. In this paper, the influence of microstructure on strength and toughness of the micrograined WC-Co hardmetal under investigation is discussed.

2. EXPERIMENTAL DETAILS

To obtain the test-pieces used in this work, the powder mixture was obtained by adding 3.5 wt.% Co to submicron WC powders (FSSS = 0.8 μm). For this purpose, 230 kg of the raw powders were ball-milled for 150 h, using solcol solvent as protecting liquid. The pressing lubricant added was liquid paraffin whereas the grain growth inhibitor used was VC. A small amount of carbon powder was also added in order to avoid WC decarburization during the subsequent stage of sintering. After milling the powder slurries were dried and sieved. Green compacts in parallelepipedic form (50 mm x 100 mm x 18 mm) were produced by uniaxial pressing at 25 MPa. Compacts were debinded and presintered in a Sinter-Vac furnace under vacuum to remove the pressing lubricant at a maximum temperature of 750°C. In order to measure flexural strength, several test-pieces were machined from the pre-sintered bars which were then sintered in a sinter-HIP. In the sinter-HIP process, low pressure hot isostatic pressing (up to 7 MPa) is combined with vacuum sintering, and the pressure is applied at the sintering temperature at which the Co-binder is still molten. Some of the test-pieces were subsequently treated according to the conditions described in Table 1. Prior to re-sintering, the test-pieces were treated with carbon powder in order to avoid decarburization of WC.

Table 1. Post-sintering conditions used.

Treatment designation	Temperature [°C]	Pressure [MPa]	Number of test-pieces treated
As-sintered	1460	2	21
Re-sinterHIP	1460	3	21
HIP	1320	100	8

After the sinter-HIP, the bars were ground using a 1 μm diamond grinding wheel (average surface roughness, R_a of 0.05 μm) and the edges were bevelled at 45° using a diamond grinding wheel, so that chamfers with 0.15 mm width were created. Prior to mechanical testing, the as-sintered test-pieces were manually polished using different diamond grits (7 and 3 μm, respectively) to a surface roughness R_a of 0.02 μm. For comparison purposes, 6 as-sintered test-pieces grinded mechanically were also tested.

The sintered density was measured by the Archimedes' method according to ISO 3369 [11] and compared to the estimated value obtained for the composite using the rule of mixtures (15.37 $g \cdot cm^{-3}$).

Polished cross-sections of the as-sintered samples were observed on an optical microscope with a magnification of 150x in order to classify their porosity according to ISO 4505 standard [12] and on a Philips XL30 FEG scanning electron microscope coupled with an energy dispersive X-ray (EDX) analyser for qualitative elemental analysis using both secondary electrons (SE) and back-scattered electrons (BSE) modes. Prior to examination, the samples were polished with a series of diamond pastes to 1 μm finish. After polishing, the samples were etched with a Murakami aqueous solution. The grain size of the hardmetal under investigation was then measured by the linear intercept method (Heyn´s method), from images obtained at a magnification of 2000x, according to the ASTM E112-96 standard [13]. By measuring the length of random intercepts an average grain size was calculated. For each field, the number of intercepts per unit length of test line N_L was calculated according to:

$$N_L = N_i / (L/M) \quad (1)$$

where N_i is the number of intercepts with a total test line length L = 500 mm and M the magnification (20000x). The mean lineal intercept value for each field l is given by the inverse of N_L.
The ASTM grain size number, G, was determined according to the equation:

$$G = (-6.643856 \log_{10} l) - 3.288 \quad (2)$$

The 95% confidence interval, 95%CI, of the measurement was calculated according to:

$$95\%CI = \frac{t\,s}{\sqrt{n}} \quad (3)$$

where n is the number of fields measured (8 for each image), t the Student's multiplier for determination of CI, and s the standard deviation.

The percent relative accuracy, %RA, was determined according to the equation:

$$\%RA = \frac{95\%CI}{\bar{X}} \cdot 100 \quad (4)$$

where:

$$\bar{X} = \frac{\sum X_i}{n} \quad (5)$$

The flexural strength was measured by three-point bending according to the ISO 3327 standard [14]. The distance between the external roller pins was 15.0 mm. All the tests were carried out in a Zwick Roell Z20 testing machine using a 0.5 mm·min^{-1} crosshead displacement speed. Load versus displacement graphs were recorded for each bar and flexural strength (modulus of rupture), σ_r, calculated assuming that stresses and deformations remain in the elastic range using the equation:

$$\sigma_r = \frac{3(F_r S)}{2(b h^2)} \quad (6)$$

where F_r is the maximum recorded load and S the outer span (15 mm). The dimensions b (width) and h (height or thickness) of each bar were measured prior to testing (with an accuracy of ± 0.02 mm).

It is known that the strength distribution of a set of brittle test samples does not follow a normal distribution. Because failure occurs at a critical flaw, it can be described by the weakest link theory. A probability function that describes the strength distribution of brittle materials is the Weibull function. The set of flexural strength data was therefore analysed using the two-parameter Weibull statistics. The Weibull modulus, m, gives an indication of the degree of scatter in fracture stress data; the higher the m value the lower is the scatter of the σ_r data. In this work, m was estimated using the maximum likelihood method according to the ASTM C1239-06A standard [15].

Once an indentation load (P) is selected and a Vickers indentation is made, the Vickers hardness (HV) can be calculated in accordance to ISO 3878 [16], using the average value for the length of the two diagonal lines of the resulting trace, according to the equation:

$$HV = 1.8544 \frac{P}{(2a)^2} \quad (7)$$

Testing was carried out at 294 N (30 kgf) using a standard hardness machine Instron-Wolpert with a Vickers diamond indenter.

The determination of the fracture toughness was made from direct measurements of the crack lengths at the four corners of a Vickers hardness indentation [17]. In comparison with more conventional testing techniques, the indentation method offers a unique simplicity and economy in test procedure. The critical stress intensity factor more commonly referred to as fracture toughness (measure of a material resistance to crack propagation) was calculated using the equilibrium relation for K-field generated by the elastic-plastic contact of a Vickers indentation on a brittle material for radial crack geometry, according to the following equation:

$$K_{Ic} = 0.0889 \left(\frac{HV \cdot P}{L_i} \right)^{1/2} \quad (8)$$

where HV is the Vickers hardness, P the indentation load and L_i the sum of the surface crack lengths of the traces emanating from the corners of the indentation (see Fig.1). This technique is suited to toughness evaluation on a comparative basis. However, it requires that the surface must be prepared to an optical finish in order that crack sizes may be accurately measured.

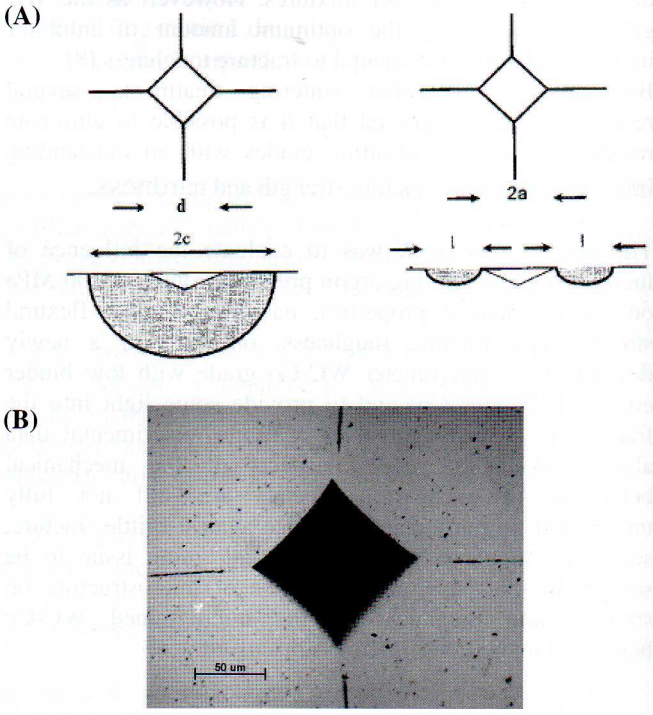

Fig. 1. Scheme showing median/half-penny (left) and radial/Palmqvist (right) crack geometries produced by a Vickers indentation (A). The optical micrograph on the right shows evidence of Palmqvist crack geometry (B).

Precautions need to be taken in selecting an indentation load, which satisfies the requirement that the pattern being well developed (c>>2a, with 2a being the dimension of the hardness impression) and that no chipping occurs. To establish the crack geometry, indented samples were polished repeatedly, using 6 μm diamond as abrasive. Once we observed that the cracks were no longer emanating from the corners of the Vickers indentation (Fig. 1B), we concluded that the crack geometry was Palmqvist-type rather than half-penny one.

3. RESULTS AND DISCUSSION

By observing the polished surface of the test-pieces (at a magnification of 1500x), it can be seen that this grade contains type A porosity (*i.e.* pore size < 10 μm), which can be attributed to the submicron grain sizes of WC as well as to the small amount of Co-rich eutectic liquid present at the

sintering temperature (Co lakes appear with a brighter contrast in Fig. 2). Increasing the argon pressure from 2 to 100 MPa has resulted in a decrease in porosity from A04B00C00 (for as-sintered test-pieces) to A02B00C00 and <A02B00C00 (for re-sinterHIP and HIP-treated test-pieces, respectively). The use of higher argon pressures has induced a more efficient rearrangement of WC grains, compacting tightly among themselves, thereby contributing to porosity reduction. Although density did not vary much with the increasing argon pressure, since a value of 15.10±0.1 g·cm^{-3} was obtained, the estimated total porosity decreased slightly from about 2 vol% (at 2 MPa) to about 1 vol% (at 100 MPa).

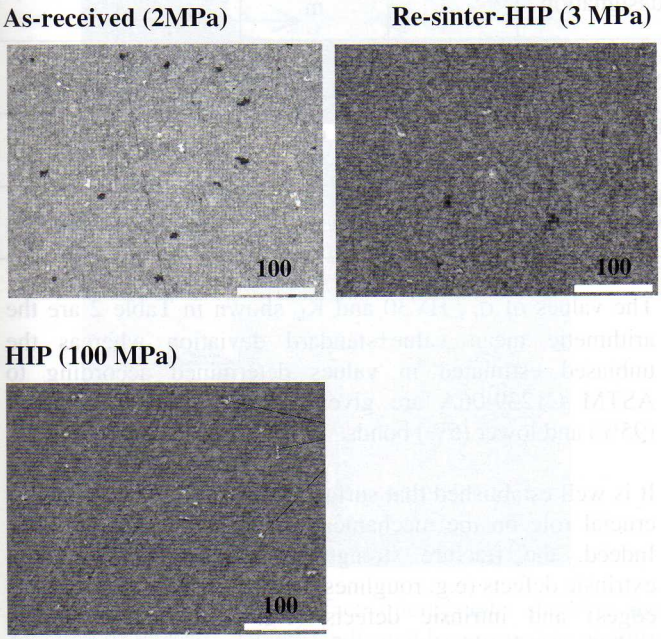

Fig. 2. Optical micrographs showing porosity evolution as a function of argon pressure.

The WC grain size for the as-sintered test-pieces was determined to be ASTM G=20, by the linear intercept method using SEM images as those shown in Fig. 3, which corresponds to an average grain size of 0.27± 0.02 µm, with 95% CI of 0.02 and the percent relative accuracy of 7.4%. For the HIP- treated test-pieces, the results obtained were average grain size of 0.28± 0.03 µm, with 95% CI of 0.02 and the percent relative accuracy of 7.1%. In spite of the fact that the average grain size did not change as a result of the post-sintering treatment, it was evident that locally a few larger grains were observed in the microstructure of the HIP-treated test-pieces as compared to the as-sintered ones (this is particularly evident in the etched cross-sections shown in Fig. 5). The main disadvantage of this grain size determination method is that the resulting values refer to measurements from one dimension (linear intercept) and that the calculations are based on the number of grains observed. As can be seen in Fig. 3, it is not always straightforward to define grain boundaries and therefore some difficulties in the determination of the grain size were experienced. A transformation of the 1D data to 3D can be done, assuming a spherical shape, by using the correction factor (1.5) proposed by Fullman [18]. The calculated 3D average grain size is 0.41 µm. From these data, it may be inferred that the grain growth inhibitor used (VC) was very effective in limiting normal and abnormal grain growth during both sintering and post-sintering heat-treatments.

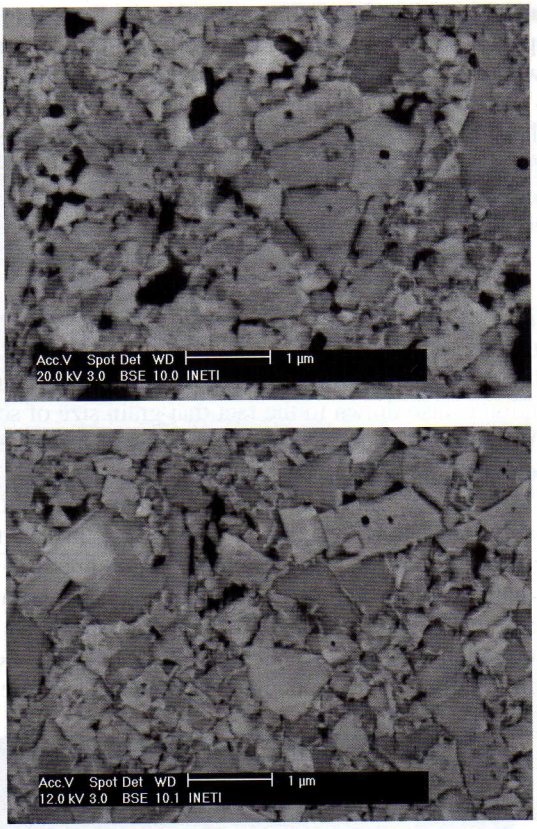

Fig. 3. Typical SEM micrographs of as-sintered (top) and HIP-treated (bottom) polished cross-sections.

The mechanism responsible for grain growth inhibition is still a matter of controversy, but it is likely that VC segregation at WC-Co grain boundaries promotes the formation of more facetted and hence less mobile WC-Co interfaces [9] as clearly shown in Fig. 4. Some of these prismatic grains contain sharp edges, which may form local tensile stress concentrations upon loading of this composite.

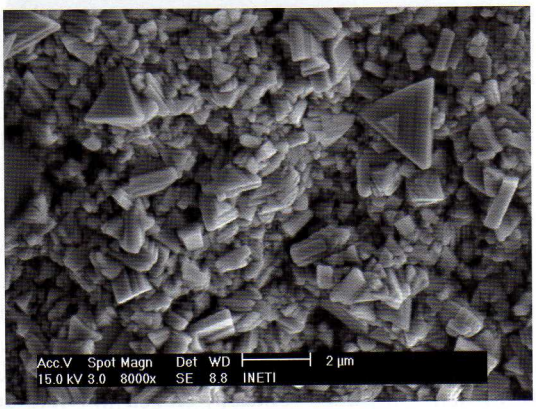

Fig. 4. Typical fracture surface of as-sintered test-piece showing prismatic grains (truncated trigonal prisms) with sharp edges.

On the other hand, increasing the argon pressure has resulted in a decrease in pore size as well as "pore clusters" size (Fig. 5). This is attributed to cobalt plastic deformation causing rearrangement of WC grains and the partial collapse of the pore structure. Due to the fact that this hardmetal only contains about 6 vol% Co, the amount of liquid phase formed upon sintering was apparently not enough to allow complete removal of the residual porosity. In addition, it is known that VC reduces the affinity and migration of Co onto WC particles thereby explaining the higher porosity levels in WC/Co/VC grades when compared to WC/Co/Cr_3C_2 ones [19]. In the case of the HIP-treated test-pieces, a similar pattern (so-called "pore cluster") is observed (see Fig. 5). In fact, the amount of liquid phase that forms at 1320ºC is expected to be considerably lower than that at 1460ºC, and thus rearrangement due a better distribution of the cobalt phase, driven by capillary forces, is most likely to prevail. This would also account for the rather small effect of the re-sintering treatment on grain growth. Attention is also drawn to the fact that grain size of some of the WC grains present in the microstructure of the HIP-treated test-pieces is of the same order of magnitude of the pore size. This indicates that the flexural strength has probably reached a maximum value for this particular material even if further increase in the argon pressure would eventually result in a slight decrease in pore size. In fact, the presence of the larger WC grains would act as tensile stress concentration defects which would likely become responsible for fracture upon loading of this composite.

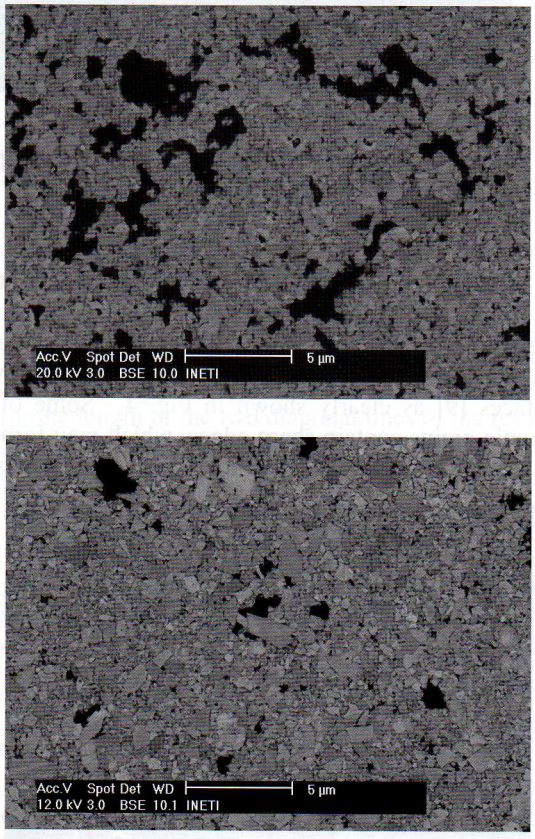

Fig. 5. Typical microstructure of as-sintered test-pieces (top) and HIP-treated test-pieces (bottom) etched in Murikami's solution.

Table 2 summarizes the mechanical properties of the material under investigation. There is a clear effect of argon pressure on the flexural strength whereas its influence on both hardness and fracture toughness is trivial. The large scatter in flexural strength is typical of brittle materials. Quality and integrity of surface finish resulting from machining are also of critical significance.

Table 2. Mechanical properties of as-received and post-sintered hardmetals.

Treatment designation	σ_r [MPa]	Weibull modulus m	HV30 [kgf·mm^{-2}]	K_{Ic} [MN·m$^{-3/2}$]
As-sintered (2 MPa)	1305±322	$4.4\ {}^{5.9}_{3.2}$	2002±35	7.6±0.2
Re-sinter HIP (3 MPa)	1552±306	$6.7\ {}^{9.1}_{5.0}$	2016±27	7.5±0.1
HIP (100 MPa)	2915±189	$14.6\ {}^{24.7}_{8.8}$	2032±8	7.8±0.1

The values of σ_r, HV30 and K_{Ic} shown in Table 2 are the arithmetic mean value±standard deviation whereas the unbiased estimated m values determined according to ASTM C1239-06A are given together with their upper (95%) and lower (5%) bonds.

It is well established that surface finishing conditions play a crucial role on the mechanical failure of hardmetals [20]. Indeed, the fracture strength is dependent upon both extrinsic defects (e.g. roughness, surface cracks, flaws, sharp edges) and intrinsic defects (e.g. pores, large grains, inclusions). In this case, surface defects introduced during the grinding operation were smaller than the intrinsic ones thereby not having any significant effect on the mechanical failure of the hardmetal under investigation. In the case of as-received test-pieces tested without further polishing, we obtained σ_r= 1568 ± 294 MPa (m= $4.8\ {}^{9.2}_{2.6}$), which clearly indicates that extrinsic flaws did not play an important role in the fracture process. Typical fracture surfaces are shown in Fig. 6. Characteristic features observed in polycrystalline materials known as mirror, mist, hackle and crack branching can also be seen in Fig. 6. None of the observed fracture surfaces showed evidence that the test-pieces failed as a result of extrinsic defects. Indeed, optical observations of the morphology of the fracture surfaces revealed that the origin of failure was usually located either close to the surface or in the bulk of the test-pieces. In the case of the HIP-treated test-pieces, it was not possible to identify the origin of failure owing to the fact they broke into several fragments. However, taking into account the results obtained it is most likely that the flexural strength data were also not affected by surface finishing. In addition, the increase in mean flexural strength from 1305 to 1552 MPa, obtained for the as-sintered and the re-sinterHIP-treated test-pieces respectively, is most likely related to processing variability rather than post-sintering treatment being effective in removing some of the critical defects. Even so, it is clear

that exposure of the as-received test-pieces to the re-sinter-HIP treatment at 3 MPa has resulted in a slight improvement of flexural strength as also indicated by the increase in Weibull modulus from 4.4 to 6.7 (see Table 2).

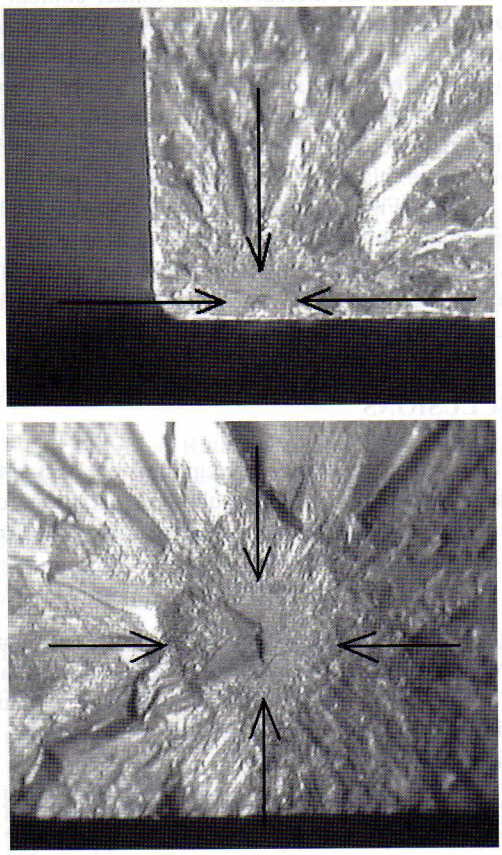

Fig. 6. Typical fracture surface micrographs showing the location of intrinsic defects (indicated by arrows) in vicinity of the surface (top) and in the bulk of as-sintered test-pieces (bottom).

Fractographic studies carried out by means of SEM and optical microscopy pointed out that the main fracture origin seems to be internal pores as shown in Fig. 7. The presence of such pores is processing-related (e.g. poor mixing, resulting in uneven distribution of the sintering aid, inappropriate debinding treatment resulting in entrapped gases).

It is well established that the fracture strength of brittle materials, σ_r, is related to the fracture toughness, K_{Ic} and the size of the critical origin defect, c, according to the Griffith's equation:

$$\sigma_r = Y K_{Ic} c^{-\frac{1}{2}} \quad (9)$$

where Y is a dimensionless proportionality factor depending on the crack geometry (Y= 1.77 [21] when c* >> a*, where c* and a* are the length and width of the defect) and c the critical size of the defect. Taking into account the values of σ_r and K_{Ic} listed in Table 3, one obtains c values ranging from 2 to 32 μm, depending upon treatment conditions. This is in good agreement with the observations made by fractography. As shown in Fig. 5, the so-called "pores clusters" are larger in the as-sintered test-pieces than in the HIP-treated ones. There is an excellent agreement between the experimental and predicted values in the case of the HIP treatment. This also accounts for the larger unbiased estimate of Weibull modulus shown in Table 2. Note that the relatively large confidence bounds associated with this estimation of m is only related to the small size of the HIP-treated test-pieces population.

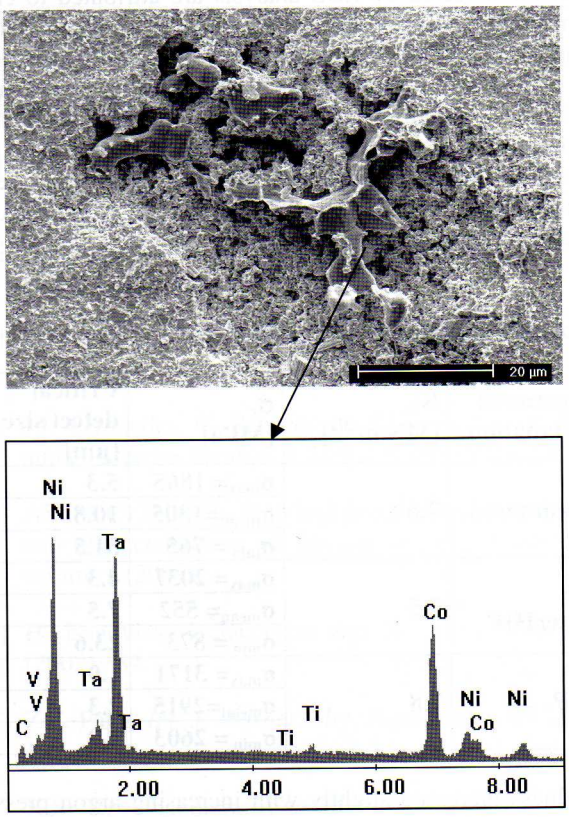

Fig. 7. Typical intrinsic defect (top) seen on the fracture surface of a as-received test-piece which broke at σ_r=1323 MPa together with EDS spot analysis (bottom) performed on the deformed Co phase.

It is known that the Co phase contains significant amounts of W and C in a solid solution and deforms extensively thus absorbing the energy by plastic deformation. This requires significant stretching of Co normal to the plane of crack propagation, and consequent contraction in order to maintain volume conservation during deformation. Evidence of considerable stretching and subsequent failure by void nucleation in Co is well documented and can be seen clearly in Fig. 7.

In the case of the as-sintered test-pieces, a wide range of critical size defects is obtained (from 5 to 32 μm). This is in line with the observations made by SEM of the defects apparent on the microstructure of polished cross-sections. In fact, Fig. 5 suggests that the size of the so-called "pores clusters" is of the order of 20 μm, which falls within the range determined using Griffith's equation. Nonetheless, the size of the defect shown in Fig. 7 reveals three intriguing features. Firstly, large deformation of the Co-rich phase is apparent. Such lakes were not observed in Fig. 5, suggesting

that some of the pores seen can be attributed to removal of the Co-phase during metallographic preparation. Indeed, there is a large difference in hardness between the WC grains and the Co phase and therefore it is possible that pull out of Co-phase during grinding and polishing may have occurred. Future work should address this issue. Secondly, it is clear that contamination introduced during the mixing of the raw powders took place. Neither Ni, Ti nor Ta were added to this grade and therefore the traces of these metallic elements detected by EDS analysis are attributed to either wear of the milling media or inadequate cleaning procedures adopted. Finally, the presence of such Co lakes suggests that the mixing step requires further optimization. Since only 6 vol% of Co is present in this grade, it is rather difficult to distribute it homogeneously throughout the fine WC particles. This indicates that alternative mixing processes to ball-milling should be sought if materials with improved mechanical strength are demanded.

Table 3. Estimated critical defect sizes.

Treatment designation	K_{Ic} [MN·m$^{-3/2}$]	σ_r [MPa]	Critical defect size [μm]
As-sintered	7.6	σ_{max}= 1865	5.3
		σ_{mean}=1305	10.8
		σ_{min} = 765	31.5
Re-sinterHIP	7.5	σ_{max}= 2037	4.3
		σ_{mean}= 552	7.5
		σ_{min} = 873	23.6
HIP	7.8	σ_{max}= 3171	1.9
		σ_{mean}=2915	2.3
		σ_{min} = 2603	2.9

Hardness increased slightly with increasing argon pressure from 2 to 100 MPa, as it can be seen in Table 2. These values are lower than the expected HV value of about 2300 kgf·mm^{-2} from the available literature [22], for a grade having 6 vol% (≈ 3.5 wt%) of Co and a mean WC grain size of 0.4 μm. The presence of residual pores is regarded as the main reason for the hardness values being lower than the predicted ones. However, it is clear that higher argon pressures resulted in a small increase in hardness as a result of some porosity removal.

No significant changes on fracture toughness values were observed with increasing argon pressure. Slight differences may be attributed to crack length measurement errors, since it is rather difficult to identify the origin and end of the cracks by means of optical microscopy.

Fracture toughness values shown in Table 2 are in good agreement with the value (8 MN·m$^{-3/2}$) reported in literature for a HV30 = 2050 kgf·mm^{-2} grade [23]. Fracture in WC-Co hardmetals with high volume fraction of Co has been found to occur mainly by plastic rupture of Co through void nucleation and coalescence [24]. However, other fracture modes including fracture along the WC-Co interface and WC-WC grain boundary decohesion as well as cleavage across WC grains may also take place, particularly at low volume fractions of Co at which the contiguity of WC grains increases. Not surprisingly, the mean fracture toughness obtained at P=294 N of 7.6 MPa·m½ approaches the value of 7.2 MPa·m½ which corresponds to the theoretical WC/WC interface toughness [25]. In general, fracture toughness increases with volume fraction of Co, the mean free path length (thickness) of the binder, and the size of WC grains. Indeed, an increase in Co binder content would minimize the fracture along the weak WC-WC boundaries, thus increasing fracture toughness. In this particular case, the content of Co binder is rather small (6 vol%) to enable all WC grains being surrounded by the Co binder phase suggesting that densification occurs mainly by solid state diffusion. This explains (i) the appearance of more prismatic carbide grains (Fig. 4), owing to the formation of low-energy prismatic interfaces, and (ii) the presence of residual porosity. The inevitable increase in WC contiguity causes a decrease in ductility and a lower toughness than that obtained for grades with higher binder contents.

4. CONCLUSIONS

The influence of argon pressure applied on post-sintering mechanical behaviour of a new submicron grade hardmetal containing 3.5 wt% Co has been studied. The main findings can be summarised as follows:

- Higher argon pressures in re-sintering this material improved flexural strength from near 1500 MPa (at 3 MPa) to about 3000 MPa (at 100 MPa), which is attributed to a reduction of the amount and size of its critical defects.
- Hardness and fracture toughness data obtained were hardly affected by argon pressure applied in post-sintering treatments.
- VC addition, by virtue of its high solubility and mobility in the Co-phase, has proven to be effective in inhibiting WC grain growth at HIP temperatures as high as 1320°C. This is also a good indication that the gross carbon content of this grade has been handled properly, otherwise local abnormal growth would have occurred.
- SEM analysis of the fracture surfaces revealed that all the examined test-pieces failed by intrinsic rather than extrinsic defects, suggesting that surface finishing had no effect on the flexural strength measurements. Hence, a smooth mechanical polishing (1μm grinding wheel) is sufficient to guarantee that the fracture of this material occurs through intrinsic (bulk) defects, since the defects arising from finishing operations are smaller than the intrinsic ones.
- Residual pores are regarded to be the major fracture origin source, although at low argon pressure, the presence of large metallic inclusions containing Co and V together with Ni, Ti and Ta impurities should also not be disregarded.
- Palmqvist radial cracks were induced by indentation using a 294 N load applied by a Vickers diamond indenter.
- Hot isostatic pressing has been demonstrated as an efficient method for obtaining submicron grained hardmetals with good abrasive wear resistance, high

strength (3 GPa), high hardness (20 GPa) but relatively low fracture toughness (7.6 MPa·m½).

ACKNOWLEDGEMENTS

The technical assistance provided by Dr. Filipe Oliveira (flexural strength measurements) from the Department of Ceramics and Glass Engineering and CICECO of the University of Aveiro is gratefully acknowledged.

REFERENCES

[1] W.D. Schubert, A. Bock and B. Lux, B., *Int. J. Refract. Met. Hard Mater.* **13** (1995) 281.

[2] W.D. Schubert, H. Neumeister, G. Kinger and B. Lux, *Int. J. Refract. Met. Hard Mater.* **16** (1998) 133.

[3] V. Richter, M.v. Ruthendorf, *Int. J. Refract. Met. Hard Mater.*, **17** (1999) 141.

[4] G. Gille, B. Szesny, K. Dreyer, H. van den Berg, J. Schmidt, T. Gestrich and G. Leitner, *Int. J. Refract. Met. Hard Mater.* **20** (2002) 3.

[5] P.V. Krakhmalev, T.A. Rodil and J. Bergström, *Wear* **236** (2007) 240.

[6] K. Brookes, *Met. Powd. Report* **60** (2005) 24.

[7] L. Zhang, G. Liu, G. Yang, S. Chen, B. Huang and C. Zhang, *Int. J. Refract. Met. Hard Mater.* **25** (2007) 166.

[8] C.H. Allibert, *Int. J. Refract. Met. Hard. Mater.* **19** (2001) 53.

[9] I. Azcona, A. Ordóñez, J.M. Sánchez and F. Castro, *J. Mat. Sci.* **37** (2002) 4189.

[10] J.M. Sánchez, A. Ordóñez and R. González, *Int. J. Refract. Met. Hard Mater.* **23** (2005) 193.

[11] ISO 3369, Impermeable sintered metal materials and hardmetals - Determination of density (2006).

[12] ISO 4505, Hardmetals - Metallographic determination of porosity and uncombined carbon (1978).

[13] ASTM E112-96, Standard test methods for determining average grain size (1996).

[14] ISO 3327, Hardmetals - Determination of transverse rupture strength (1982).

[15] ASTM C1239-06A, Standard practice for reporting uniaxial strength data and estimating Weibull distribution parameters for advanced ceramics (2007).

[16] ISO 3878, Hardmetals - Vickers hardness test (1983).

[17] D.K. Shetty, I.G. Wright, P.N. Mincer and A.H. Clauer, *J. Mat. Sci.* **20** (1985) 1873.

[18] H. Engqvist, B. Uhrenius, *Int. J. Ref. Met. & Hard Mat.* **21** (2003) 31.

[19] D.F. Caroll, *Int. J. Refract. Met. Hard Mater.* **17** (1999) 123.

[20] J.J. Fernandes, C. Pacheco da Silva, L. Guerra Rosa and C. Martins Saraiva, *J. Mat. Sci.* **29** (1994) 2008.

[21] ASTM C1322-05b, Standard practice for fractography and characterization of fracture origins in advanced ceramics (2007).

[22] H. Engqvist, S. Jacobson and N. Axén, *Wear* **252** (2002) 384.

[23] Z.Z. Fang, *Int. J. Refract. Met. Hard Mater.* **23** (2005) 119.

[24] K.S. Ravichandran, *Acta Metall. Mater.* **42** (1994) 143.

[25] N. Sacks, C. Allen and I. Northrop, Proceedings of the Powder Metallurgy World Congress & Exhibition, Granada, Spain, October 18-22, 1998, European Powder Metallurgy Association Vol. **4** (1998), p. 8.